Full Articles

Boron chelate complexes: X-ray and UV photoelectron spectra and electronic structure*

S. A. Tikhonov★ and V. I. Vovna

Far Eastern Federal University,
8 ul. Sukhanova, 690950 Vladivostok, Russian Federation.
Fax: +7 (423) 265 2225. E-mail: allser@bk.ru

Published data on the electronic structure of boron chelates are summarized for the first time. Ultraviolet photoelectron spectra of vapors, X-ray photoelectron spectra of molecular crystals, and results of modeling within the framework of the density functional theory are analyzed. Data on the effect of substituents on the electronic structure of complexes are systematized.

Key words: electronic structure, photoelectron spectroscopy, density functional theory, boron chelate complexes.

Boron chelate complexes are finding increasing use in various fields of science and technology. For instance, boron β-diketonates exhibit intense luminescence throughout the visible and near-IR regions,[1—6] the ability to form excimers[7,8] and exciplexes,[9,10] luminescent thermochromism,[11] liquid-crystalline polymorphism,[12—15] and high biological activity.[16] These properties underlie the application of the title compounds as laser dyes,[17] organic light-emitting diodes,[18,19] optical chemosensors,[20—22] active components of sunlight collectors,[23] nonlinear optical materials,[24] polymeric optical materials,[25,26] and antiviral drugs.[16] Much attention is also attracted to nitrogen-containing analogues of boron β-diketonates. In particular, unique photophysical properties of boron imidoylamidinates and formazanates offer prospects for their application in the design of novel laser dyes.[27—31] Specific properties[32—35] of boron difluoride dipyrrolylmethene (BODIPY) complexes allow one to expect that materials based on BODIPY and their derivatives may serve as active components of light harvesters,[36] biomolecular probes,[37] and optical chemosensors.[38]

Establishment of correlations between the electronic structure and spectral characteristics of boron chelates makes targeted synthesis of novel optical materials feasible. Absorption spectroscopy was the main physical method of investigation of the electronic structure before 1970s; however, the dependence of the energy of electronic transitions on the energy of two electronic levels limits the informativeness of the method. Photoionization causes electrons to go to the ground-state level, which simplifies

* Based on the materials of the XXVII International Chugaev Conference on Coordination Chemistry (October 2—6, 2017; Nizhny Novgorod, Russia).

Published in Russian in *Izvestiya Akademii Nauk. Seriya Khimicheskaya,* No. 7, pp. 1153—1166, July, 2018.

the interpretation of the photoelectron spectra within the framework of the MO approximation and thus makes ultraviolet photoelectron spectroscopy (UPS) and X-ray photoelectron spectroscopy (XPS) reliable sources of information on filled electronic levels.[39] Photoelectron spectra of coordination compounds often exhibit broad bands that cannot be interpreted without using modern computational methods.

The choice of the density functional theory (DFT) to model the electronic structure of boron chelate complexes is due to good correlation between the experimental and theoretical ionization energies of d-element coordination compounds.[40—42] This can be explained by similarity between the Kohn—Sham equation and the Dyson quasiparticle equation for valence ionization.[43,44] The general Dyson equation[45] is a way to obtain Green′s functions;[46] therefore, utilization of the DFT approach that takes account of electron correlation in polyatomic systems made it possible to interpret the broad bands in the UPS and XPS spectra.

The electronic structure and optical properties of boron chelates have been intensively studied by optical spectroscopy and quantum chemistry methods. Compounds of interest include boron difluoride β-diketonates (they can be synthesized with relative ease), boron difluoride β-diketonates bearing organic substituents at boron, and their nitrogen-containing analogues. Photoelectron spectra of certain boron chelate complexes were reported earlier.[47,48] However, at that time the available methods for electronic structure calculations of polyatomic systems failed to unambiguously establish the nature and order of electronic levels. Except Ref. 49, all results of photoelectron spectroscopy studies of boron chelate complexes were reported in our publications.

In this work we briefly review the results of UPS, XPS, and DFT studies on the electronic structure of certain classes of boron β-diketonate complexes and their nitrogen-containing analogues (**A**—**C**) carried out in the last decade at the Laboratory of Electronic Structure and Quantum Chemical Modeling (Far Eastern Federal University, Russia). We studied the effect of substituents at β-position of the chelate ring on the electronic structure of boron difluoride β-diketonates. Replacement of two fluorine atoms by various organic groups made it possible to determine the role of the complex-forming agent in the changes in the MO energies and composition. Studies on boron imidoylamidinates and formazanates disclosed the electronic effects originating from substitution of various organic groups in α-, β-, and γ-positions, as well as heteroatoms in the chelate and fused rings. The results obtained[50—64] are compared with absorption spectroscopy data and with the results of time-dependent density functional theory (TDDFT) calculations.[52,58,62,63]

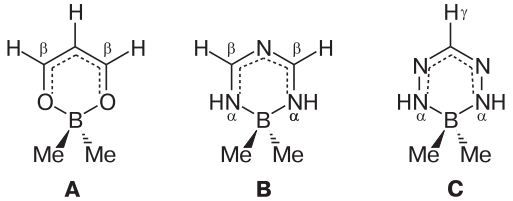

Experimental

Methods of synthesis of boron difluoride β-diketonates, boron difluoride β-diketonates with organic substituents at boron atoms, and their nitrogen-containing analogues have been analyzed in Refs 65, 66, and 67, respectively.

Vapor-phase UPS spectra of 30 boron chelates were registered on a modified ES-3201 electron spectrometer with a hemispherical electrostatic analyzer and a monochromatic He I radiation source ($h\nu$ = 21.2 eV).[47,48,57,59,60,63] To calibrate the electron energy scale, xenon was used. The error in the determination of band maxima was at most 0.08 eV. The temperature of the ionization cell was varied from 200 to 240 °C depending on the properties of the samples.

Broad bands in the UPS spectra were decomposed into Gaussian components taking account of the calculated number of electronic levels, the energy intervals between them, and the relative photoionization cross-sections. Correlations between the experimental bands and the energies of calculated electronic levels were made using a procedure similar to extended version of Koopmans′ theorem[68], *viz.*, $I_i = -\varepsilon_i + \delta_i$, where I_i is the ionization energy, ε_i is the one-electron Kohn—Sham energy, and δ_i is the density functional approximation defect (DFA defect) representing a measure of deviation of the one-electron energy ε_i from the experimental vertical ionization energy I_i.

X-ray photoelectron spectra of molecular crystals of 11 boron β-diketonates were recorded on a high-vacuum photoelectron spectrometer (Omicron, Germany) with hemispherical electrostatic analyzer and a source of Mg-Kα radiation ($h\nu$ = = 1253.6 eV).[52,54,58,62,63] The instrument function of the spectrometer in the mode of characteristic atomic levels registration, determined from the $Ag3d_{5/2}$ band shape, had a half-width of 1.2 eV. The spectra were processed using the CASA XPS software.[69] The electron binding energy (E_b) scale was calibrated using the F1s (686.0 eV) or C1s (285.5 eV) levels as internal standards.[70,71] The atomic concentrations of elements in the samples were determined taking account of the relative ionization cross-sections and the photoelectron escape depth. The relative concentrations of elements obtained from the 1s-electron band intensities coincided with the calculated values within the limits of experimental error (10%).

The valence-region and core-level XPS spectra were interpreted using the frozen orbital approximation. This allowed one to make a qualitative assignment of the energy subbands in molecular crystals to the calculated energies taking into account the number of calculated electronic levels, the energy intervals between them, and the relative ionization cross-sections.

Density functional calculations were carried out using the Firefly program[72] with basis sets of at least 6-311G quality.[73,74] The results of calculations depend strongly on the exchange-correlation functional chosen. At present, DFT calculations use hybrid functionals,[75] doubly hybrid functionals,[76] Minnesota functionals,[77] and hybrid range-separated functionals.[78,79] Besides, the method of dispersion correction is used as an add-

on to conventional Kohn—Sham technique.[80] The B3LYP hybrid functional[81—83] is successfully used in modeling the electronic structure and optical spectra of boron chelate complexes.[84—90] It was shown that B3LYP calculations give good agreement between theory and experiment for the structure and spectral characteristics of boron chelates (see our review[56] and Ref. 91). Therefore, all UPS and XPS spectra were compared with the results of DFT calculations using the B3LYP functional. The absorption spectra of the complexes were interpreted in accordance with the results of TDDFT calculations.

Results and Discussion

Boron difluoride β-diketonates. Presented below are the results of UPS (see Refs 50—54, 63) and XPS (see Refs 58, 62, 63) studies of the electronic structure of 18 boron difluoride β-diketonates and the results of corresponding DFT calculations. For these complexes we analyzed the results of calculations and absorption spectroscopy data.

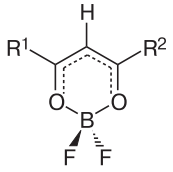

1—18

Compound	R^1	R^2
1	Me	Me
2	Ph	Me
3	*p*-Tol	Me
4	*p,m*-MeC_6H_3	Me
5	4-Biphenyl	Me
6	4-Fluorenyl	Me
7	4-*trans*-Stilbenyl	Me
8	2-Naphthyl	Me
9	9-Anthryl	Me
10	Ph	Ph
11	*p*-$OMeC_6H_4$	*p*-$OMeC_6H_4$
12	*p*-$OMeC_6H_4$	*m*-$NO_2C_6H_4$
13	*p*-$OMeC_6H_4$	*p*-$NO_2C_6H_4$
14	$C_{10}H_7$	*p*-$NO_2C_6H_4$
15	*p*-Tol	*p*-Tol
16	*p*-$OMeC_6H_4$	Ph
17	*p*-$OMeC_6H_4$	*p*-BrC_6H_4
18	*p*-$OMeC_6H_4$	*o*-$OHC_6H_3COOC_6H_4OMe$

Boron difluoride acetylacetonate F_2BAcac (**1**) is one of the best studied β-diketonates. The structure of compound **1** has a C_{2v} symmetry. The HOMO of the complex is a π-orbital mainly localized on the Cγ atom and two O atoms (Fig. 1). The n_-MO has a large contribution from oxygen AOs (58%). Orbitals mainly composed of F2p AO have lower energies[50] and can be treated as a result of mixing of the chelate ring MOs with symmetry types a_1, b_1, and b_2 with corresponding orbitals of the complex-forming agent F_2B.[47,48]

To determine how the F_2B orbitals affect the electron density distribution in the ligand π-MOs and n_O-AOs, we performed a comparative analysis of the electronic structure of lithium acetylacetonate[92] and boron difluoride acetylacetonate[50] using UPS data and results of DFT calculations. As the Li atom in the acetylacetonate complex is replaced by F_2B, the I_1 and I_2 values increase by 1.60 and 2.24 eV, respectively. This can be explained by a decrease in the total electron density on the ligand from −0.64 *e* in LiAcac to −0.13 *e* in F_2BAcac since the boron atom donates the electron density mainly to two fluorine atoms (0.74 *e*) rather than oxygens.

The first two bands in the UPS spectrum of F_2BAcac originate from one-electron ionization from the π_3 and n_ MOs (see Fig. 1, Table 1). Broad asymmetric band shapes at 9.85 and 11.34 eV with a half-width of 0.6 eV are indicative of significant changes in the geometry of the ion upon removal of electrons from the π- and *n*-orbitals.[50]

To interpret the third band in the spectrum of F_2Bacac, we compared[50] the I_i and ε_i values of the following compounds: BF_3, BF_2Me, $CH_2{=}CF_2$, C_2H_6, benzene and its derivatives $C_6H_{6-n}R_n$ (n = 1, 2; R = F, Me, OH), complexes $M(AA)_n$ (n = 1—3; M = Be, Zn, Sc). It was found that the DFA defect for the levels mainly composed of carbon AOs (δ_C) is 2.0—2.2 eV. For MOs with major compositions of O2p and F2p AOs, the DFA defect is 0.2—0.4 and 1.0—1.5 eV higher, respectively. Therefore, the DFA defect for the valence MOs of boron difluoride acetylacetonate, mainly composed of carbon (oxygen) AOs is δ_C = 2.0 eV (δ_O = 2.4 eV), while that for the levels with major composition of F2p AOs is δ_F = 3.4 eV. A similar ratio of the DFA defect values was also found for other boron difluoride β-diketonates. Thus, the third band in the UPS spectrum of F_2BAcac (see Fig. 1) corresponds to the n_+-MO and three nonbonding F2p AOs. Earlier,[47,48] the band at 12.8 eV was assigned to the n_+-orbital since at that time computational methods did not allow the I_i energy of F2p levels to be so low. It was accepted that the I_i energies of F2p electrons lower 13 eV are only characteristic of metal fluorides with mainly ionic bonding.[93]

The HOMOs of compounds **2**—**4** with one benzene ring as substituent are composed of π_3 orbital and the upper degenerate orbital of benzene e_{1g}, while methylation of the phenyl group decreases the ionization energies of not only the substituent π-orbitals, but also the chelate ring π-orbitals[50] (see Table 1). Unlike compounds **2**—**4**, substituents in complexes **5—7** have an extended π-system. Therefore, one or two upper occupied orbitals in systems **5—7** are mainly localized on the aromatic group, while the π_3 orbital makes the major contribution to the second or third higher occupied MO.[51] The UPS spectra of boron difluoride naphthaloylacetonate (**8**) and boron difluoride anthracenoylacetonate (**9**) exhibit a fine structure of the spectral bands corresponding to I_1, which is due to the C=C-bonding π-orbitals localized on substituents,[63] by analogy with the naphthalene[94] and anthracene[95] molecules. The difference between theoretical and experimental I_1 values of boron difluoride dibenzoylmethanate

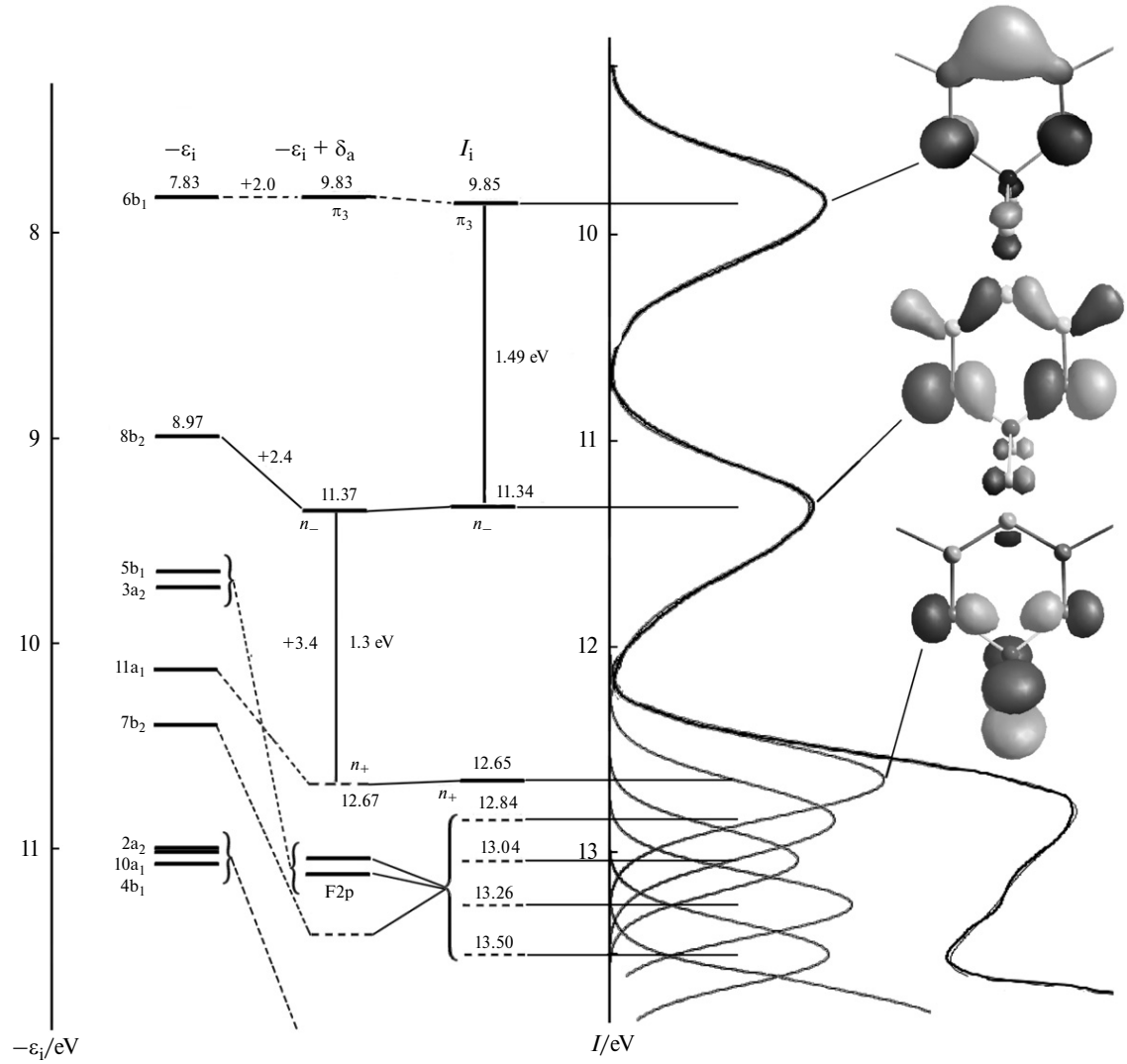

Fig. 1. UPS data and energy diagrams for F_2BAcac: calculated electron energies (ε_i), those corrected for the DFA defect (2.0, 2.4, and 3.4 eV for the π_3, n, and F2p orbitales, respectively), and the experimentally determined (including the results of spectral decompositon of the third band) energies I_i.[50]

Table 1. Experimental and calculated ionization energies (eV) of different MOs in compounds **1**—**10**[50—52,63]

Compound	R_1		R_2		$\pi_3 - R_3$		R_3		R_4		$R_3 + \pi_3$		R_5		n_	
	$-\varepsilon_i + \delta_i$	I_i	$-\varepsilon_i + \delta_i$	I_i	$-\varepsilon_i + \delta_i$	I_i	$-\varepsilon_i + \delta_i$	I_i	$-\varepsilon_i + \delta_i$	I_i	$-\varepsilon_i + \delta_i$	I_i	$-\varepsilon_i + \delta_i$	I_i	$-\varepsilon_i + \delta_i$	I_i
1	—	—	—	—	9.83	9.85	—	—	—	—	—	—	—	—	11.37	11.34
2	—	—	—	—	9.30	9.25	9.67	9.82	—	—	10.06	10.16	—	—	11.08	11.14
3	—	—	—	—	9.09	9.02	9.59	9.67	—	—	9.85	9.96	—	—	10.99	10.93
4	—	—	—	—	8.99	8.85	9.31	9.27	—	—	9.76	9.73	—	—	10.85	10.83
5	8.82	8.81	—	—	9.49	9.48	9.50	9.49	7.77	9.77	10.36	10.35	—	—	11.01	11.00
6	8.40	8.29	9.13	9.19	9.29	9.33	9.47	9.55	—	—	10.30	10.31	—	—	10.77	10.76
7	8.07	8.15	—	—	9.12	9.10	9.24	9.34	9.50	9.50	9.83	9.78	10.92	10.80	10.71	10.77
8	8.50	8.40	—	—	9.02	9.03	—	—	—	—	9.62	9.64	10.36	10.40	10.84	10.92
9	7.58	7.56	8.88	8.70	9.16	9.20	—	—	—	—	9.43	9.49	10.48, 10.58	10.22, 10.45	10.64	10.64
10	—	—	—	—	9.19	9.00	9.83	9.85	9.99	10.10	10.27	10.35	—	—	11.17	11.12

Note. No mixing of π_3 and R_3 orbitals in compound **1**; π_3 and n_ are the chelate ring orbitals, and R_1—R_5 are orbitals localized on substituents at the β-position. Here and in Tables 2—5 the plus (+) and minus (−) signs respectively denote bonding and antibonding between the chelate ring and substituent.

F_2BDbm (**10**) is 0.19 eV. Calculations of I_1 from the total energy differences between the ionized state and the ground state predict significant rearrangements in the electron shell upon removal of an electron from the HOMO.[52]

We compared the results of UPS and DFT studies on the electronic structure of compounds **1**—**10** with the absorption spectroscopy data and results of TDDFT calculations.[52,58,96] It was found that the energy and oscillator strength of the n—π* transition remain almost unchanged, whereas those of π—π* transitions vary from one compound to another. This especially concerns the oscillator strength values that are maximum for the π_3—π_4* transitions (complexes **3** and **10**), for the R—π_4* transitions (complexes **2**, **5**—**7**, **9**), and for the second transition R—π_4* (complexes **4** and **8**).

Among boron chelate complexes, boron difluoride dibenzoylmethanate F_2BDbm (**10**) deserves particular attention since it exhibits high photostability, bright luminescence in solution,[97] in the crystalline phase,[98] and in polymer matrices.[99] Spectral characteristics of F_2BDbm and its derivatives are intensively studied in connection with great potential for practical applications. In particular, the dependence of the orbital energy on location (*o*-, *m*-, or *p*-position) of the OMe substituent in alkoxy-substituted F_2BDbm was studied.[100,101] The results of theoretical studies of a large number of boron chelate complexes were reviewed[102] with the emphasis placed on the choice of the method for implicit inclusion of the solvent effect. The influence of substitution of methoxy and alkyl groups in *p*-position of the benzene rings of F_2BDbm on its luminescence spectra was studied.[103,104] The results of theoretical analysis of the fine structure in the optical spectra of F_2BDbm (see Ref. 105) and its hydroxylated derivative were reported.[106]

The valence region XPS spectra of compounds **10**—**18** exhibit four or five maxima in the E_b range of 3 to 23 eV and two maxima in the range of 27—31 eV (Fig. 2). The relative intensities and band shapes are governed by the distribution of the density of electronic states and by the relative ionization cross-sections of s- and p-levels (σ_s and σ_p, respectively). For Mg-Kα radiation, the $\sigma_s : \sigma_p$ ratio equals 26 for carbon, 12 for oxygen, 4 for fluorine, and 0.5 for bromine; note that $\sigma_p(C) : \sigma_p(O) : \sigma_p(F) : \sigma_p(Br) = 1.0 : 6.0 : 19.6 : 113.0$.[107]

A thorough analysis[52] of the valence region XPS spectrum of F_2BDbm (see Fig. 2) showed that maxima in the energy range of 10—22 eV correlate with the benzene orbitals $2a_{1g}$, $2e_{1u}$, $2e_{2g}$, and $2b_{1u}$. Maxima at 31 and 27 eV are due to ionization from the F2s and O2s levels, respectively. The difference between the experimental data for the

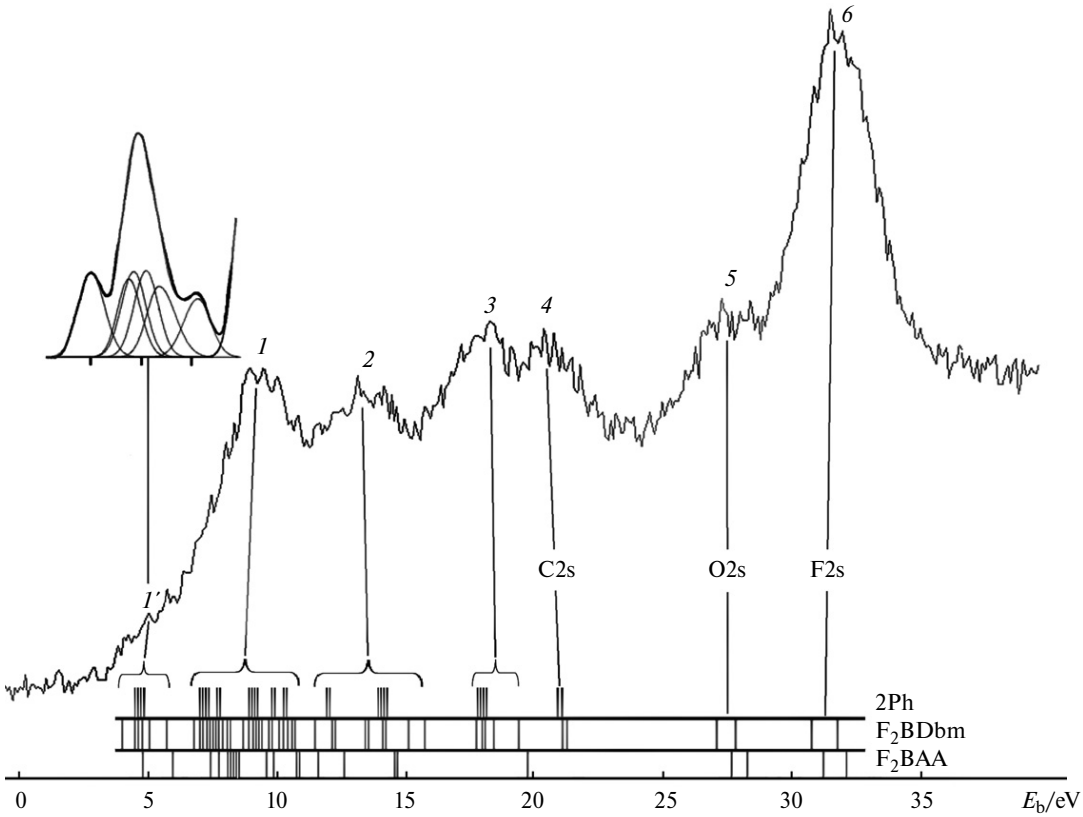

Fig. 2. Valence-region XPS spectrum of F_2BDbm (see Ref. 52) and calculated electron energies of three compounds. Lines corresponding to the O2s and F2s electron energies are respectively shifted by 1 and 3 eV relative to other levels. A weak bend 1′ corresponds to six upper occupied MOs observed in the vapor-phase UPS spectrum (its scale is magnified: ×2).

ionization intensities of O2s and F2s levels in the spectrum of F_2BDbm originates from not only errors of the computational method used to evaluate the photoionization cross-sections of free atoms, but also from delocalization of the electron density over the chelate ring.[52] In particular, both O2s-type orbitals in F_2BDbm are the O—C bonding ones, which is also characteristic of compounds **11**—**18**.[58,62]

Figure 3 presents the C1s and O1s XPS spectra of compounds **15**—**18** and the calculated energies responsible for the half-widths and positions of maxima of 1s-electron bands on the E_b scale. By analogy with F_2BDbm (see Ref. 52) the C1s spectra of complexes **11**—**18** exhibit two components, C1s and C1s′, while the satellite at 289 eV is called "π-plasmon"[108] and associated with π —π* excitation of aromatic groups[109] (shake-up p_z transition).

Bands in the O1s spectra of compounds **16**—**18** shown in Fig. 3 were decomposed into components in accordance with results of calculations. Similarly to other boron difluoride β-diketonates,[54,63] the binding energies of B1s-electrons in complexes **10**—**18** are in the range of

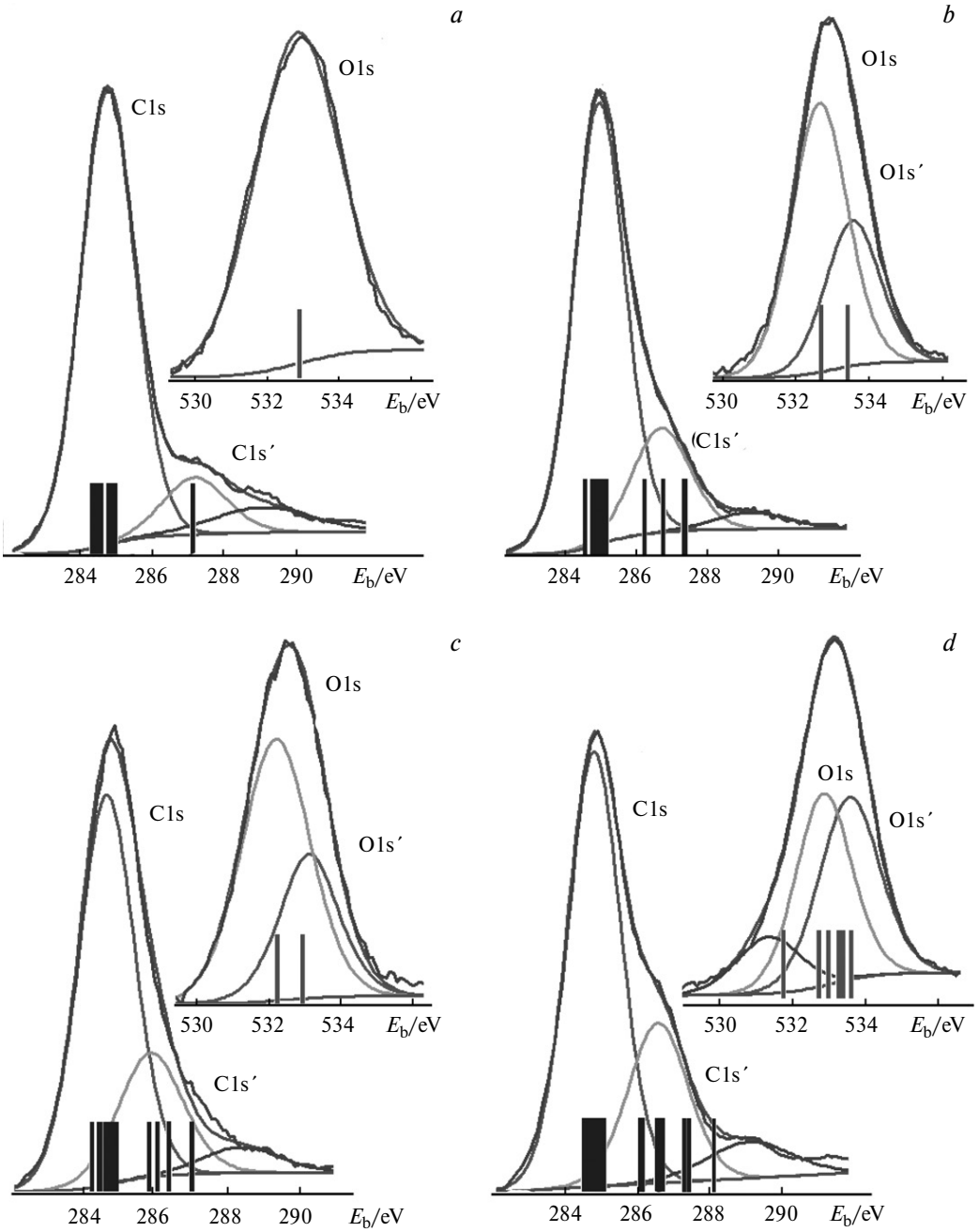

Fig. 3. C1s and O1s XPS spectra of compounds **15** (*a*), **16** (*b*), **17** (*c*), and **18** (*d*).[62]

193.6—193.8 eV. According to reference data,[107] this is characteristic of B atom in high oxidation states. The core-level XPS spectra of complexes **10**—**18** demonstrate good agreement between the energy differences and the relative areas under Gaussians with the calculated energies and the number of electronic levels.

Boron β-diketonates with organic substituents. In the text below we present the results of electronic structure studies[53,54] of five β-diketonates **19**—**23** with organic substituents at boron. For compounds **21**—**23** we also analyzed the results of calculations and absorption spectroscopy data.[110]

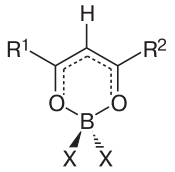

19—23

$R^1 = R^2$ = Me, X = Et (**19**); $R^1 = R^2$ = Me, X = Ph (**20**);
$R^1 = R^2$ = Me, 2X = $C_6H_4O_2$ (**21**);
R^1 = Ph, R^2 = Me, 2X = $C_6H_4O_2$ (**22**);
$R^1 = R^2$ = Ph, 2X = $C_6H_4O_2$ (**23**)

Calculations predict that, unlike F_2Bacac, complexes **19**—**21** are characterized by significant mixing of the ligand π_3 MO with orbitals localized on the organic substituents at boron (Table 2). As a consequence, the HOMO—LUMO energy gap becomes narrower and the nature of the S_0—S_1 transition changes.

It was found that compound **21** has MOs mainly localized on O atoms of the $C_6H_4O_2$ moiety.[53] Two upper electronic levels in spiroborates **21**—**23** are localized on the $C_6H_4O_2$ fragment while replacement of Me groups by Ph in the β-diketonate ring has almost no effect on the energies and localization of the two higher and deeper-lying π- and σ-orbitals of $C_6H_4O_2$ (see Ref. 54, Table 2, Fig. 4). Replacement of two fluorine atoms by $C_6H_4O_2$ in complexes **1**, **2**, and **10** has no effect on the energies and composition of π-levels of the β-diketonate ligand (see Fig. 4, Tables 1 and 2). The lack of mutual perturbation of electronic levels of two chelate rings in spiroborates can be explained by the fact that their planes are mutually orthogonal.

The first three bands in the UPS spectra of compounds **21**—**23** (Fig. 5) are due to one-electron ionization. In the spectra of complexes **21**—**23** the energies I_1 and I_2 are determined by two upper π-MOs (π_5^X and π_4^X) of $C_6H_4O_2B$ moiety representing the antibonding combinations of two upper π-orbitals of the phenylene ring ($1e_{1g}$ in benzene) with O2p AOs. The third band corresponds to the π_3 MO of chelate ring (compound **21**) or to the antibonding combination π_3 MO – R (compounds **22** and **23**). It is followed by broad bands assigned to a number of electronic levels.[54]

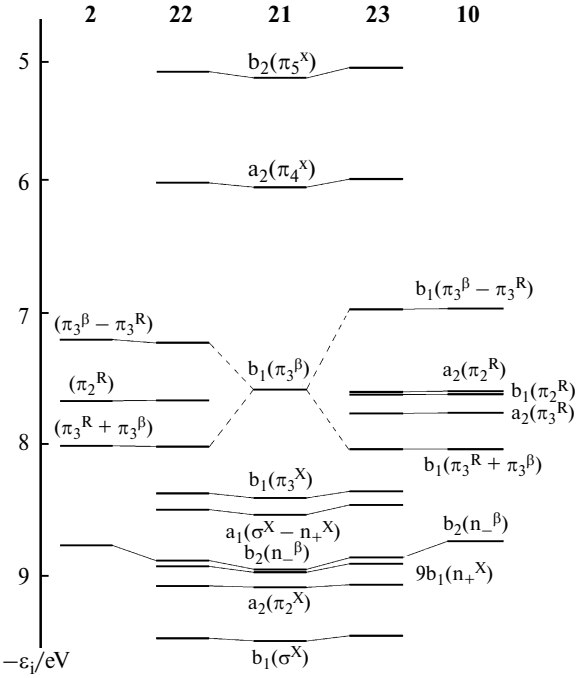

Fig. 4. Correlation diagram for interaction of upper π- and σ-MOs in compounds **21**—**23**, F_2Bbac (**2**), and F_2BDbm (**10**).[54]

The results of calculations are in good agreement with the UPS spectra. Considering compound **21**, of nine upper electronic levels with $I < 12$ eV, only two are localized on the β-diketonate moiety (see Figs 4 and 5, Table 2). According to calculations, the strong band with a maximum at 11.3 eV and a shoulder at 10.6 eV should be decomposed into six Gaussians including the n_-MO, two π-orbitals mainly localized on the $C_6H_4O_2B$ group, and three n- and σ-MOs.[54]

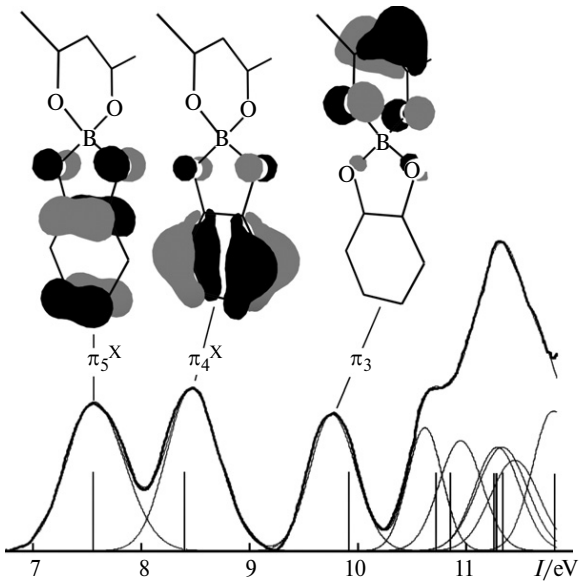

Fig. 5. UPS spectrum of compound **21**.[54] Shown are the MO shapes of the first three spectral bands.

Table 2. Experimental and calculated ionization energies (eV) of different MOs in compounds **19**—**23**[53,54]

Compound	X_1		X_2		$\pi_3 - X_3$		$X_3 + \pi_3$		R		$R + \pi_3$		X_3		n_		X_4		$X_5 + n_-$	
	$-\varepsilon_i + \delta_i$	I_i	$-\varepsilon_i + \delta_i$	I_i	$-\varepsilon_i + \delta_i$	I_i	$-\varepsilon_i + \delta_i$	I_i	$-\varepsilon_i + \delta_i$	I_i	$-\varepsilon_i + \delta_i$	I_i	$-\varepsilon_i + \delta_i$	I_i	$-\varepsilon_i + \delta_i$	I_i	$-\varepsilon_i + \delta_i$	I_i	$-\varepsilon_i + \delta_i$	I_i
19	—	—	—	—	8.41	8.50	9.85	9.79	—	—	—	—	10.10	10.14	10.45	10.42	10.79, 10.84	10.75, 10.82	—	—
20	8.31—8.81	8.36—8.83	—	—	9.13	9.07	10.43	10.31	—	—	—	—	—	—	10.78	10.64	10.92, 11.00	10.92, 11.13	11.28	11.39
21	7.55	7.56	8.39	8.47	9.93	9.76	—	—	—	—	—	—	10.74, 10.87	10.63, 10.95	11.29	11.29	11.31—11.83	11.34—11.81	—	—
22	7.54	7.52	8.38	8.45	9.33	9.29	—	—	9.77	9.81	10.12	10.12	10.47, 10.59	10.46, 10.67	10.98	10.94	11.03, 11.17,	10.99, 11.24	—	—
23	7.51	7.45	8.36	8.34	8.90	8.85	—	—	9.53, 9.70	9.64, 9.82	9.97	9.91	10.28, 10.39	10.14, 10.34	10.79	—	—	—	—	—

Note. No mixing of π_3 and X_3 orbitals in compounds **21**—**23**; π_3 and n_ are the chelate ring orbitals, R are orbitals localized on substituents at β-position, and X_1—X_5 are orbitals of organic groups at boron atom.

Table 3. Experimental and calculated ionization energies (eV) of different MOs in compounds **24**—**27**[55,59,61]

Compound	$\pi_3 - X$		$R - \pi_3$		$R - X$		R		$X - R$		$n_- + X$		$R + \pi_3$		n_N		$X + \pi_3$		$X + n_N$	
	$-\varepsilon_i + \delta_i$	I_i	$-\varepsilon_i + \delta_i$	I_i	$-\varepsilon_i + \delta_i$	I_i	$-\varepsilon_i + \delta_i$	I_i	$-\varepsilon_i + \delta_i$	I_i	$-\varepsilon_i + \delta_i$	I_i	$-\varepsilon_i + \delta_i$	I_i	$-\varepsilon_i + \delta_i$	I_i	$-\varepsilon_i + \delta_i$	I_i	$-\varepsilon_i + \delta_i$	I_i
24	7.84	7.75	—	—	—	—	—	—	—	—	—	—	—	—	9.42	9.41	9.65	9.66	9.80	9.87
25	7.75	7.59	—	—	—	—	9.01—9.25	8.86—9.23	—	—	—	—	—	—	9.49	9.44	9.71	9.56	9.73	9.67
26	—	—	8.50	8.32	9.14, 9.22	9.07, 9.33	9.39	9.37	9.50, 9.59	9.47, 9.70	9.70	9.78	10.23	10.12	—	—	—	—	—	—
27	—	—	8.09	7.84	9.21, 9.35	9.20, 9.30	9.29—9.52	9.30—9.58	9.64, 9.72	9.70, 9.80	9.75	9.85	10.50	10.40	—	—	—	—	—	—

Note: π_3, n_N, and n_ are the chelate ring orbitals, R are orbitals localized on substituents at α-, β-, and γ-positions, and X are orbitals of organic groups at boron atom.

The valence region XPS spectra of complexes **21** and **23** exhibit five maxima (Fig. 6). The relative intensities and the shape of spectral components are determined by the distribution of the density of electronic states and by the relative ionization cross-sections of the 2s and 2p levels (σ_s and σ_p, respectively). According to reference data,[107] for Mg-Kα radiation the $\sigma_s : \sigma_p$ ratio equals 26 for carbon and 12 for oxygen at $\sigma_p(C) : \sigma_p(O) = 1 : 6$.

Maxima *5* in the spectra of both complexes (see Fig. 6) correspond to two pairs of electronic levels mainly localized (to 80%) on O atoms. The half-width of the band is 4.7 eV, being in good agreement with theoretical estimate of the splitting of four levels by 3.46 eV.

Maximum *4* and a bend *4′* in the spectrum of compound **21** originate from electrons of three C2s levels ($3a_1$, $2b_2$, $5a_1$) of acetylacetonate ligand and three levels, namely, $4a_1(a)$, $2b_1(e_1)$, $6a_1(e_1)$ of the C_6H_4 ring (see Fig. 6). Maximum *3* at 14.5 eV corresponds to two levels, $8a_1(e_2)$ and $3b_1(e_2)$, of the C_6H_4 group and to the $3b_2$ level of the

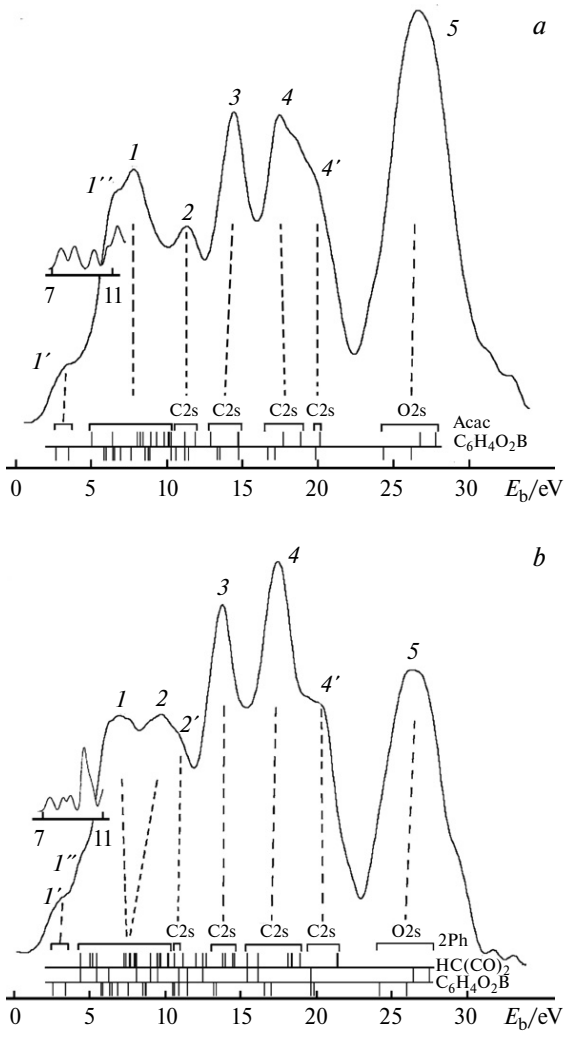

Fig. 6. Valence-region UPS and XPS spectra of compounds **21** (*a*) and **23** (*b*) (for details, see text).[54]

β-diketonate ligand. Maximum *2* at 11.3 eV is determined by the upper s-MO (out of six ones) of the C_6H_4 group. Maximum *1* and bends *1′* and *1′′* correspond to ionization from 22 p-levels including four n_O orbitals and eight π orbitals. The first two bands in the vapor-phase UPS spectrum (see Fig. 5) appear in the XPS spectrum of condensed state as a bend *1′* near the top of the filled energy band, while the strong maximum at 11.3 eV composed of the contributions from six orbitals corresponds to bend *1′′*. Superimposition of the vapor-phase UPS spectra on the valence region XPS spectra confirms the assignment of the bends (see Fig. 6).

Replacement of two methyl groups by phenyl moieties (compound **23**) leads to an increase in the number of electronic levels in the valence region from 41 to 63 (the number of s-levels increases from 16 to 26). Since the total number of O atoms remains unchanged, the relative intensities of maxima *1*—*4* in the spectrum increased (see Fig. 6). The bend *4′* and maximum *4* correspond to the a and e_1 electron levels of three benzene rings and C atoms of the β-diketonate ligand.[54] Maximum *3* is due to contributions from three pairs of e_2 orbitals, while maxima *1* and *2* correspond to 38 p-levels and three 2s levels. By analogy with the spectrum of compound **21** bend *1′* corresponds to the first two bands, while bend *1′′* corresponds to the strong band at 9.8 eV in the vapor-phase UPS spectrum.

The results of experimental and theoretical studies of the absorption spectra of compounds **21**—**23** are available.[110] Replacement of two F atoms by $C_6H_4O_2$ moiety leads to a change in the nature of the S_0—S_1 transition and to a bathochromic shift of the long-wavelength band owing to a decrease in the HOMO—LUMO gap. These data are in good agreement with the results of analysis of the electronic structure of boron difluoride β-diketonates and spiroborates (see Fig. 4).

Six-membered nitrogen-containing analogues of boron β-diketonates. In the text below we present the results of electronic structure studies of two boron imidoylamidinates[55] and two boron formazanates.[59]

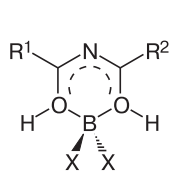

24, 25

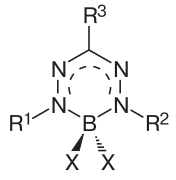

26, 27

$R^1 = R^2$ = Et, X = MeCOO (**24**); $R^1 = R^2$ = Ph, X = MeCOO (**25**); $R^1 = R^2$ = Ph, R^3 = H, X = Ac (**26**); $R^1 = R^2$ = Ph, R^3 = *p*-Tol, X = Ac (**27**)

According to calculations, compounds **24** and **25** are characterized by mixing of the chelate ring π_3 MO and orbitals of the complex-forming agent X (Table 3). Unlike **25**, strong mixing of the chelate π-MO and benzene ring

π-MO was found for complexes **24** and **27**; this is also typical of boron β-diketonates.[50—52,54] Inter-orbital interaction causes the I_1 energy of complex **26** to increase by 0.73 eV relative to that of **25** (see Table 3). Introduction of tolyl group at γ-position of chelate ring (compound **27**) leads to noticeable delocalization of the upper occupied MOs. In complex **27** mixing of the chelate ring π_3 MO with the π_3 orbital of *p*-Tol group is responsible for a decrease in I_1 by 0.48 eV compared to compound **26**. According to UPS data, additional π-orbitals of toluene cause the splitting of the π_3 level to increase by 0.76 eV.

Figure 7 presents the UPS spectra of complexes **25**—**27** decomposed into Gaussian components. Vertical lines denote the calculated electron energies corrected for the DFA defect. A comparison of the results of simulation and the UPS spectra revealed good agreement between theory and experiment.[59]

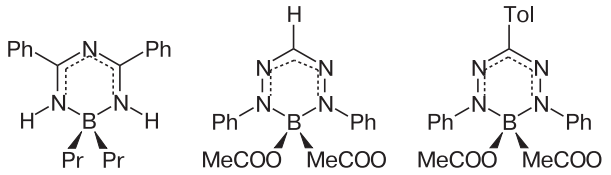

25 **26** **27**

The UPS spectra of compounds **25**—**27** exhibit broad bands corresponding to I_1 (see Fig. 7), which is determined by the set of components for $3N$–6 vibrations; this is also characteristic of boron β-diketonates.[50—54] In accordance with the Franck—Condon principle, photoionization from the HOMO causes noticeable changes in the equilibrium coordinates due to the stretching and deformation vibrations. For complexes **25**—**27**, the energy differences between the vertical and adiabatic transition are in the range of 0.58—0.87 eV.

Gaussian components of the UPS spectra of compounds **25**—**27** (see Fig. 7) are asymmetric; this is also characteristic of the valence orbitals of benzene,[111] heterocyclic compounds,[112], boron β-diketonates,[50—54] and their nitrogen-containing analogues. For compounds **25** and **27**, the asymmetry parameters of the I_1 band (the right/left half-width ratio) are 1.12 and 1.10, respectively. The overlap of the first and second bands in the spectrum of complex **26** makes the determination of the asymmetry parameter difficult.

Boron imidoylamidinates with fused rings. Now we will analyze the results of electronic structure studies of compounds **28**—**35**.[55,57]

By analogy with boron acetylacetonates with organic substituents[53] complexes **28**—**35** are characterized by noticeable mixing of the ligand and complex-forming agent MOs (Table 4) and by correlation of the shapes of five upper occupied MOs. Methylation of the benzene ring at the *m*-position (compound **31**) leads to considerable changes in the localization and energies of the fourth, fifth, and sixth upper occupied MOs.[55]

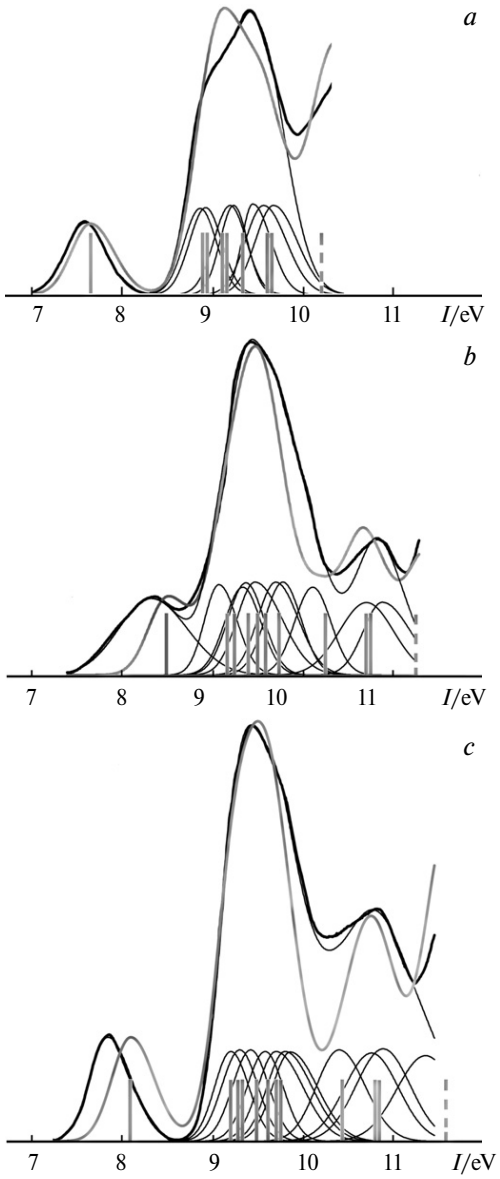

Fig. 7. Vapor-phase UPS spectra of compounds **25** (*a*), **26** (*b*), and **27** (*c*) (black solid lines). Gray solid lines denote the results of simulation.[59]

Boron imidoylamidinates **29**—**31**, **33**, and **35** exhibit no marked mixing of the ligand and phenyl group π-orbitals (see Tables 3 and 4). Complexes **29**—**31** demonstrate an increase in the I_i values for phenyl group levels by 0.4—1.1 eV compared to complex **25**. This can be explained by the field effect of the positive charge on the six-membered ring (0.47 *e*) donating the electron density to the five-membered ring.

In complexes **28**—**35** there are five π-MOs of the chelate ring, one pseudo-π-orbital of the complex-forming agent X, and one (compounds **32**—**34**) or two (compounds **28**—**31**) n_N MOs. The first bands in the UPS spectra of **28**—**35** originate from one-electron ionization from the π_5-X MO (see Table 4).

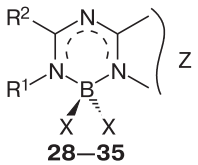

28—35

Compound	X	Z	R^1	R^2
28	Pr	=N–CH=N–	H	H
29	Pr	=N–CH=N–	H	Ph
30	Pr	=N–CH=N–	H	*p*-Tol
31	Pr	–N–CH=N–	H	*m*-Tol
32	Bu	–S–CH=CH–	H	H
33	Bu	–S–CH=CH–	H	*p*-Tol
34	Pr	–S–CH=CH–	Cyclohexyl	Cyclohexylamine
35	Pr	–N=CH–CH=CH–	Cyclohexyl	Cyclohexylamine

Replacement of two N atoms in the five-membered ring (compounds **28—30**) by sulfur atom and CH group (complexes **32** and **33**, respectively) causes I_1 to decrease by 0.2—0.3 eV (see Table 4). In compound **33** the electronic levels of the benzene ring orbitals R are 0.8—1.2 eV higher than the corresponding levels in complex **30**.[57] This can be explained by the electron-withdrawing properties of two N atoms of the five-membered ring that displaced the electron density from the six-membered ring. Unlike boron formazanates[59] and boron β-diketonates,[50—52,54] no marked mixing between the ligand π-MO and benzene ring orbitals was found for complexes **29—31** and **33** (see Table 4).

Compounds **34** and **35** are characterized by noticeable mixing of ligand orbitals and the $C_6H_{11}NH$ group orbitals, while the presence of nitrogen atom in the fused ring (compound **35**) leads to an increase in I_1 by 0.18 eV.

Aza-boron-dipyridomethene derivatives. Let us turn to analysis of UPS data and results of DFT calculations of nitrogen-containing chelate complexes **36—38**.[60,61]

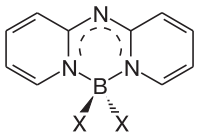

36—38

X = Et (**36**), Pr (**37**), Ph (**38**)

To assess the effect of the complex-forming agents on the electronic structure of aza-boron-dipyridomethene derivatives, we analyzed the changes in the I_i values and in the MO types on going from anthracene and acridine to structure **36** (Fig. 8). The molecules of anthracene, acridine, and compound **36** have seven occupied π-orbitals each, the HOMO being localized on three rings. Due to the field effect of two β-C atoms in structure **36** the n_N level is considerably stabilized compared to the corresponding value for acridine, which leads to an increase in the energy gap between I_1 and I_2 (see Fig. 8). Unlike aza-boron-dipyridomethene with BF_2 group (see Ref. 60), in compounds **36—38** one deals with noticeable mixing of the chelate ligand π-MO and pseudo-π-orbitals of the complex-forming agent X (Table 5). This governs the decrease in the HOMO—LUMO gap and can lead to bathochromic shift of the long-wavelength bands in the optical spectra.

Replacement of Et by Pr (complex **37**) causes no great changes in the energies and compositions of the six upper occupied orbitals. Phenyl groups in compound **38** stabilize the ligand MO levels by 0.1—0.2 eV (see Table 5). According to UPS data for compounds **37** and **38**, the level of the X—π orbital is stabilized by 0.78 and 0.74 eV, respectively, compared to complex **36**.

Complexes **36—38**, anthracene, and acridine molecules exhibit a correlation of the π_7 HOMO localized on three rings. This gives rise to a fine structure of the first bands in the vapor-phase UPS spectra of these compounds (see Fig. 8), which is due to C=C-bond vibrations.

Correlation of experimental and calculated ionization energies. The experimental ionization energies I_i (from UPS data) and the calculated electron energies ε_i of complexes **1—10** and **19—38** can be compared by shifting the energy scale by 2.04 eV (Fig. 9, *a*). Having averaged the DFA defect (δ_i) value for each complex and taking account of the dependence of δ_i on the MO localization, the average difference between the experimental and calculated I_i values for a total of 168 levels is 0.06 eV (Fig. 9, *b*) at $R^2 = 0.994$. We successfully used a similar procedure for correlating the UPS data and results of DFT calculations elsewhere.[56,61]

Table 4. Experimental and calculated ionization energies (eV) of different MOs in compounds **28—35**[55,57,61]

Compound	$\pi_5 - X$		$\pi_4 - X$		n_N		$\pi_3 + X$		X		R – X		R		$n_N - X$		n_N	
	$-\varepsilon_i + \delta_i$	I_i	$-\varepsilon_i + \delta_i$	I_i	$-\varepsilon_i + \delta_i$	I_i	$-\varepsilon_i + \delta_i$	I_i	$-\varepsilon_i + \delta_i$	I_i	$-\varepsilon_i + \delta_i$	I_i	$-\varepsilon_i + \delta_i$	I_i	$-\varepsilon_i + \delta_i$	I_i	$-\varepsilon_i + \delta_i$	I_i
28	8.17	7.99	9.16	9.24	9.43	9.53	—	—	—	—	—	—	—	—	—	—	—	—
29	7.87	7.70	8.82	8.87	9.15	9.24	9.48	9.45	9.55	9.64	9.98	—	10.00	—	—	—	—	—
30	7.75	7.66	8.69	8.65	9.03	9.14	9.35	9.30	9.43	9.52	9.66	—	9.85	—	—	—	—	—
31	7.78	7.74	8.75	8.74	9.06	9.06	9.37	9.32	9.45	9.48	9.52	9.63	9.78	—	—	—	—	—
32	7.76	7.70	9.09	9.15	—	—	—	—	—	—	—	—	—	—	—	—	—	—
33	7.61	7.50	—	—	—	—	—	—	—	—	8.63, 9.19	8.61, 9.28	9.17	9.22	—	—	—	—
34	7.05	6.97	7.89	7.88	—	—	8.66	8.80	—	—	—	—	—	—	—	—	—	—
35	7.29	7.15	8.03	7.90	—	—	—	—	—	—	—	—	—	—	8.72, 8.97	8.77, 9.01	9.05	9.22

Note. For compounds **34** and **35**, listed are the $\pi_4 - R - X$ and $R - \pi_4$ MO energies; π_3, π_4, π_5, and n_N are the chelate orbitals, R are orbitals localized on substituents at α- and β-positions, X are orbitals of organic groups at B atom.

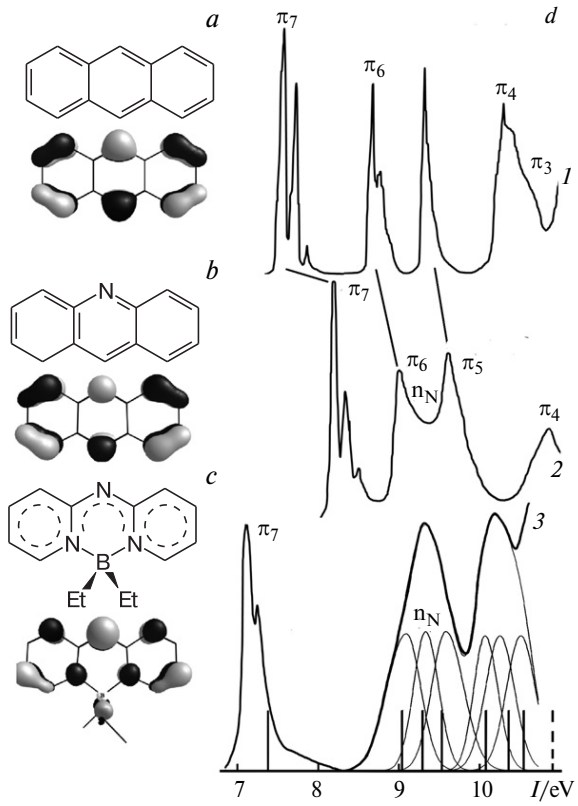

Fig. 8. HOMO shapes (*a*—*c*) and vapor-phase UPS spectra (*d*) of anthracene[95] (*1*), acridine[113] (*2*), and compound **36** (*3*).[60] Band assignment in the spectra of anthracene and acridine is based on the results of calculations.[61]

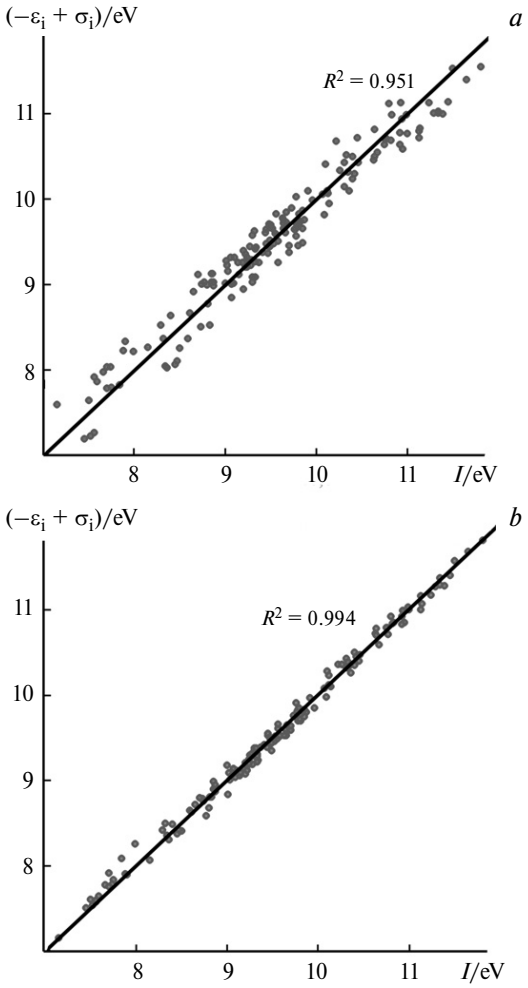

Fig. 9. Correlation between experimental and calculated ionization energies for 30 boron chelate complexes (a total of 168 energy values) using the average value of the DFA defect (δ) calculated for all compounds ($I_i = -\varepsilon_i + 2.04$ eV) (*a*) and using the δ values averaged separately for each complex and taking account of the dependence of δ_i on the MO localization ($I_i = -\varepsilon_i + \delta_i$) (*b*).

Summing up, we systematized data on the effect of substituents on the electronic structure of 38 boron chelate complexes. Considering boron difluoride acetylacetonate, benzoylacetonate, and dibenzoylmethanate, replacement of two fluorine atoms by the $C_6H_4O_2$ group has no effect on the energies and composition of π-levels of the β-diketonate ring, which can be explained by the fact that the ligand planes in spiroborates are mutually orthogonal. Owing to extended π-system of substituents in the series of boron difluoride β-diketonates containing biphenyl, fluorenyl, and *trans*-stilbenyl at carbonyl C atoms, one or two higher occupied orbitals are mainly localized on the aromatic group, while the π_3 orbital makes the major contribution to the second or third occupied upper π-MO. Unlike boron β-diketonates and formazanates, boron imidoylamidinates show no marked mixing of the chelate and benzene ring π-MOs. The presence of fused ring with N atoms causes an increase in I_1 by 0.2—0.3 eV and stabilization of the π-MO levels of phenyl group by 0.8—1.2 eV.

Table 5. Experimental and calculated ionization energies (eV) of different MO in compounds **36—38**[60,61]

Compound	π_7		X — π		X		n_N		π_6		X		π_5	
	$-\varepsilon_i + \delta_i$	I_i	$-\varepsilon_i + \delta_i$	I_i	$-\varepsilon_i + \delta_i$	I_i	$-\varepsilon_i + \delta_i$	I_i	$-\varepsilon_i + \delta_i$	I_i	$-\varepsilon_i + \delta_i$	I_i	$-\varepsilon_i + \delta_i$	I_i
36	7.37	7.11, 7.25	9.04	9.09	—	—	9.29	9.33	9.53	9.58	10.08	10.07	10.36	10.26
37	7.29	7.05, 7.25	8.95	8.87	—	—	9.20	9.24	9.44	9.49	—	—	—	—
38	7.51	7.16, 7.34	9.71	9.83	8.35—8.69	8.47—8.88	9.45	9.45	9.56	9.56	—	—	—	—

Note: π_5, π_5, and π_5 are the chelate ring orbitals and X are orbitals of organic groups at boron atom.

The first band in the UPS spectra of three aza-boron-dipyridomethene derivatives, boron difluoride naphthaloylacetonate, and boron difluoride anthracenoylacetonate exhibits a fine structure originating from C=C bond vibrations by analogy with naphthalene, anthracene, and acridine molecules. The DFT/B3LYP calculated energy intervals between electronic levels are in good agreement with experimental photoelectron spectroscopy data. This allows one to successfully use the results obtained to establish structure—property correlations.

This work was carried out within the framework of the Government Assignment under financial support from the Ministry of Education and Science of the Russian Federation (Project No. 3.2168.2017/4.6).

References

1. E. V. Fedorenko, A. G. Mirochnik, A. Y. Beloliptsev, V. V. Isakov, *Dyes Pigm.*, 2014, **109**, 181.
2. Y. Pi, D.-J. Wang, H. Liu, Y.-J. Hu, X.-H. Wei, J. Zheng, *Spectrochim. Acta, Part A*, 2014, **131**, 209.
3. Y. Suwa, M. Yamaji, H. Okamoto, *Tetrahedron Lett.*, 2016, **57**, 1695.
4. C. Liu, H. Zhang, J. Zhao, *RSC Adv.*, 2016, **6**, 92341.
5. E. V. Fedorenko, A. G. Mirochnik, A. Y. Beloliptsev, *J. Lumin.*, 2017, **185**, 23.
6. H. Zhang, C. Liu, J. Xiu, J. Qiu, *Dyes Pigm.*, 2017, **136**, 798.
7. A. G. Mirochnik, B. V. Bukvetskii, E. V. Gukhman, V. E. Karasev, *J. Fluoresc.*, 2003, **13**, 157.
8. B. V. Bukvetskii, E. V. Fedorenko, A. G. Mirochnik, A. Y. Beloliptsev, *J. Struct. Chem.*, 2010, **51**, 545.
9. Y. L. Chow, C. I. Johansson, *J. Phys. Chem.*, 1995, **99**, 17558.
10. Y. L. Chow, C. J. Johansson, *J. Phys. Chem.*, 1995, **99**, 17566.
11. A. G. Mirochnik, E. V. Fedorenko, B. V. Bukvetskii, V. E. Karasev, *Russ. Chem. Bull.*, 2005, **54**, 1060.
12. O. A. Turanova, G. G. Garifzyanova, A. N. Turanov, *Russ. J. Gen. Chem.*, 2010, **80**, 2317.
13. M. J. Mayoral, P. Ovejero, M. Cano, G. Orellana, *Dalton Trans.*, 2011, **40**, 377.
14. I. Sánchez, J. A. Campo, J. V. Heras, M. Cano, *Inorg. Chim. Acta*, 2012, **381**, 124.
15. E. Giziroglu, A. Nesrullajev, N. Orhan, *J. Mol. Struct.*, 2014, **1057**, 246.
16. A. Flores-Parra, R. Contreras, *Coord. Chem. Rev.*, 2000, **196**, 85.
17. German (East) Pat., DD/265266; *Chem. Abstr.*, 1990, **112**, 45278.
18. C. A. DeRosa, C. Kerr, Z. Fan, M. Kolpaczynska, A. S. Mathew, R. E. Evans, G. Zhang, C. L. Fraser, *ACS Appl. Mater. Interfaces*, 2015, **7**, 23633.
19. M. L. Daly, C. A. DeRosa, C. Kerr, W. A. Morris, C. L. Fraser, *RSC Adv.*, 2016, **6**, 81631.
20. L. Zhai, M. Liu, P. Xue, J. Sun, P. Gong, Z. Zhang, J. Sun, R. Lu, *J. Mater. Chem. C*, 2016, **4**, 7939.
21. A. S. Mathew, C. A. DeRosa, J. N. Demas, C. L. Fraser, *Anal. Methods*, 2016, **8**, 3109.
22. J. Samonina-Kosicka, D. H. Weitzel, C. L. Hofmann, H. Hendargo, G. Hanna, M. W. Dewhirst, G. M. Palmer, C. L. Fraser, *Macromol. Rapid Commun.*, 2015, **36**, 694.
23. German Pat. 10152938; *Chem. Abstr.*, 2003, **123**, 378622.
24. R. Kammler, G. Bourhill, Y. Jin, C. Bräuchle, G. Görlitz, H. Hartmann, *J. Chem. Soc., Faraday Trans.*, 1996, **92**, 945.
25. K. Tanaka, K. Tamashima, A. Nagai, T. Okawa, Y. Chujo, *Macromolecules*, 2013, **46**, 2969.
26. G. Zhang, R. E. Evans, K. A. Campbell, C. L. Fraser, *Macromolecules*, 2009, **42**, 8627.
27. J. Banuelos, F. L. Arbeloa, V. Martinez, M. Liras, A. Costela, I. G. Moreno, I. L. Arbeloa, *Phys. Chem. Chem. Phys.*, 2011, **13**, 3437.
28. Y. Deng, Y.-Y. Cheng, H. Liu, J. Mack, H. Lu, L.-G. Zhu, *Tetrahedron Lett.*, 2014, **55**, 3792.
29. S. M. Barbon, V. N. Staroverov, J. B. Gilroy, *J. Org. Chem.*, 2015, **80**, 5226.
30. M. Hesari, S. M. Barbon, V. N. Staroverov, Z. Ding, J. B. Gilroy, *Chem. Commun.*, 2015, **51**, 3766.
31. R. R. Maar, S. M. Barbon, N. Sharma, H. Groom, L. G. Luyt, J. B. Gilroy, *Chem. Eur. J.*, 2015, **21**, 15589.
32. R. Ziessel, G. Ulricha, A. Harrimanb, *New J. Chem.*, 2007, **31**, 496.
33. L. N. Sobenina, O. V. Petrova, K. B. Petrushenko, I. A. Ushakov, A. I. Mikhaleva, R. Meallet-Renault, B. A. Trofimov, *Eur. J. Org. Chem.*, 2013, **19**, 4107.
34. Y. S. Marfin, A. V. Solomonov, A. S. Timin, E. V. Rumyantsev, *Curr. Med. Chem.*, 2017, **24**, 1.
35. J. C. Berrones-Reyes, C. C. Vidyasagara, B. M. Muñoz Flores, V. M. Jiménez-Pérez, *J. Lumin.*, 2018, **195**, 290.
36. S. P. Singh, T. Gayathri, *Eur. J. Org. Chem.*, 2014, **22**, 4689.
37. T. Papalia, G. Siracusano, I. Colao, A. Barattucci, M. C. Aversa, S. Serroni, G. Zappala, S. Campagna, M. T. Sciortino, F. Puntoriero, P. Bonaccorsi, *Dyes Pigm.*, 2014, **110**, 67.
38. D. Gong, Y. Tian, C. Yang, A. lqbal, Z. Wang, W. Liu, W. Qin, X. Zhu, H. Guo, *Biosens. Bioelectron.*, 2016, **85**, 178.
39. S. Hüfner, *Photoelectron Spectroscopy: Principles and Applications*, Springer, Berlin, 1996, 511 pp.
40. I. V. Krauklis, V. Yu. Chizhov, *Opt. Spectrosc.*, 2004, **96**, 47.
41. I. V. Krauklis, V. Yu. Chizhov, *Opt. Spectrosc.*, 2005, **98**, 341.
42. Yu. V. Chizhov, Doctor of Science (Phys.-Math.) Thesis, St. Petersburg State University, St. Petersburg, 2009, 337 pp. (in Russian).
43. S. Hamel, P. Duffy, M. E. Casida, D. R. Salahub, *J. Electron Spectrosc. Relat. Phenom.*, 2002, **123**, 345.
44. P. Duffy, D. P. Chong, M. E. Casida, D. R. Salagub, *Phys. Rev. A: At. Mol. Opt. Phys.*, 1994, **50**, 4707.
45. E. K. U. Gross, E. Runge, O. Heinonen, *Many Particle Theory*, Adam Hilger, Bristol, 1992, 443 pp.
46. E. N. Economou, *Green's Functions in Quantum Physics*, Springer, New York, 1979, 251 pp.
47. A. V. Borisenko, V. I. Vovna, V. V. Gorchakov, O. A. Korotkikh, *J. Struct. Chem.* (*USSR*), 1987, **28**, 127.
48. A. V. Borisenko, Candidate of Science (Chem.) Thesis, Far Eastern Federal University, Vladivostok, 1990, 203 pp. (in Russian).
49. V. F. Traven, A. V. Manaev, T. A. Chibisova, *J. Electron Spectrosc. Relat. Phenom.*, 2005, **149**, 6.
50. V. I. Vovna, S. A. Tikhonov, I. B. Lvov, *Russ. J. Phys. Chem. A*, 2011, **85**, 1942.
51. V. I. Vovna, S. A. Tikhonov, I. B. Lvov, *Russ. J. Phys. Chem. A*, 2013, **87**, 688.
52. V. I. Vovna, S. A. Tikhonov, M. V. Kazachek, I. B. Lvov, V. V. Korochentsev, E. V. Fedorenko, A. G. Mirochnik, *J. Electron Spectr. Relat. Phenom.*, 2013, **189**, 116.
53. S. A. Tikhonov, I. B. Lvov, V. I. Vovna, *Russ. J. Phys. Chem. B.*, 2014, **33**, 11.
54. V. I. Vovna, S. A. Tikhonov, I. B. Lvov, I. S. Osmushko, I. V. Svistunova, O. L. Shcheka, *J. Electron Spectr. Relat. Phenom.*, 2014, **197**, 43.

55. S. A. Tikhonov, V. I. Vovna, *J. Struct. Chem.*, 2015, **56**, 446.
56. I. S. Osmushko, V. I. Vovna, S. A. Tikhonov, Y. V. Chizhov, I. V. Krauklis, *Int. J. Quantum Chem.*, 2016, **116**, 325.
57. S. A. Tikhonov, V. I. Vovna, A. V. Borisenko, *J. Mol. Struct.*, 2016, **1115**, 1.
58. S. A. Tikhonov, V. I. Vovna, N. A. Gelfand, I. S. Osmushko, E. V. Fedorenko, A. G. Mirochnik, *J. Phys. Chem. A*, 2016, **120**, 7361.
59. S. A. Tikhonov, V. I. Vovna, A. V. Borisenko, *J. Electron Spectr. Relat. Phenom.*, 2016, **213**, 32.
60. S. A. Tikhonov, V. I. Vovna, A. V. Borisenko, *J. Struct. Chem.*, 2017, **58**, 1061.
61. S. A. Tikhonov, I. B. Lvov, V. I. Vovna, *J. Struct. Chem.*, 2017, **58**, 1069.
62. S. A. Tikhonov, V. I. Vovna, I. S. Osmushko, E. V. Fedorenko, A. G. Mirochnik, *Spectrochim. Acta Mol. Biomol. Spectrosc.*, 2018, **189**, 563.
63. S. A. Tikhonov, V. I. Vovna, I. B. L´vov, I. S. Os´mushko, A. V. Borisenko, E. V. Fedorenko, A. G. Mirochnik, *J. Lumin.*, 2018, **195**, 79.
64. S. A. Tikhonov, Candidate of Science (Phys.-Math.) Thesis, Far Eastern Federal University, Vladivostok, 2013, 121 pp. (in Russian).
65. V. E. Karasev, A. G. Mirochnik, E. V. Fedorenko, *Fotofizaka i fotokhimiya* β*-diketonatov diftorida bora* [*Boron Difluoride* β*-Diketonates*, *Their Photophysics and Photochemistry*], Dalnauka, Vladivostok, 2006, 162 pp. (in Russian).
66. A. Barabas, E. Isfan, M. Roman, M. Paraschiv, E. Romas, A. T. Balaban, *Tetrahedron*, 1968, **24**, 1133.
67. L. S. Vasil´ev, S. V. Baranin, I. V. Zavarzin, *Russ. Chem. Bull.* (*Int. Ed.*), 2017, **66**, 1398.
68. U. Salzner, R. Baer, *J. Chem. Phys.*, 2009, **131**, 231101.
69. *CasaXPS Version 2.3.12*, Casa Software Ltd, 2006.
70. V. I. Vovna, V. V. Gorchakov, A. Y. Mamaev, V. E. Karasev, V. E. Kandinsky, A. G. Mirochnik, *Koord. Khimiya Rus.*, 1984, **10**, 1362.
71. D. Yu. Kosyanov, R. P. Yavetskiy, V. N. Baumer, Yu. L. Kopylov, V. B. Kravchenko, I. O. Vorona, A. I. Cherednichenko, V. I. Vovna, A. V. Tolmachev, *J. Alloys Compd.*, 2016, **686**, 526.
72. A. A. Granovsky, *Firefly version 8.1.1.G*; http://classic.chem.msu.su/gran/firefly/, 2017.
73. *Basis Set Exchange, version 1.2.2*; https://bse.pnl.gov/bse/portal/, 2017.
74. F. Jensen, *Adv. Rev.*, 2013, **3**, 273.
75. M. Marsman, J. Paier, A. Stroppa, G. Kresse, *J. Phys.: Condens. Matter*, 2008, **20**, 064201.
76. L. Goerigk, S. Grimme, *Wiley Interdiscip. Rev.: Comput. Mol. Sci.*, 2014, **4**, 576.
77. Y. Zhao, D. G. Truhlar, *Chem. Phys. Lett.*, 2011, **502**, 1.
78. A. E. Raeber, B. M. Wong, *J. Chem. Theory Comput.*, 2015, **11**, 2199.
79. A. Prlj, B. F. E. Curchod, A. Fabrizio, L. Floryan, C. Corminboeu, *J. Phys. Chem. Lett.*, 2015, **6**, 13.
80. S. Grimme, J. Antony, S. Ehrlich, H. Krieg, *J. Chem. Phys.*, 2010, **132**, 154104.
81. C. Lee, W. Yang, R. G. Parr, *Phys. Rev. B: Condens. Matter Mater. Phys.*, 1988, **37**, 785.
82. A. D. Becke, *J. Chem. Phys.*, 1993, **98**, 5648.
83. P. J. Stephens, F. J. Devlin, C. F. Chabalowski, M. J. Frisch, *J. Phys. Chem.*, 1994, **98** 11623.
84. E. V. Rumyantsev, S. N. Alyoshin, Y. S. Marfin, *Inorg. Chim. Acta*, 2013, **408**, 181.
85. D. N. Tomilin, K. B. Petrushenko, L. N. Sobenina, M. D. Gotsko, I. A. Ushakov, A. D. Skitnevskaya, A. B. Trofimov, B. A. Trofimov, *Asian J. Org. Chem.*, 2016, **5**, 1288.
86. S. N. Margar, L. Rhyman, P. Ramasami, N. Sekar, *Spectrochim. Acta*, *Part A*, 2016, **152**, 241.
87. M. Kolpaczynska, C. A. DeRosa, W. A. Morris, C. L. Fraser, *Aust. J. Chem.*, 2016, **69**, 537.
88. D. A. Merkushev, S. D. Usoltsev, Yu. S. Marfin, A. P. Pushkarev, D. Volyniuk, J. V. Grazulevicius, E. V. Rumyantsev, *Mater. Chem. Phys.*, 2017, **187**, 104.
89. H. Zhang, C. Liu, J. Xiu, J. Qiu, *Dyes Pigm.*, 2017, 136, 798.
90. A. Yu. Kritskaya, N. A. Bumagina, E. V. Antina, A. A. Ksenofontov, M. B. Berezin, A. S. Semeikin, *J. Fluoresc.*, 2018, **28**, 39.
91. G. B. Guseva, E. V. Antina, A. A. Ksenofontov, E. N. Nuraneeva, *J. Struct. Chem.*, 2016, **57**, 25.
92. A. Yu. Ustinov, M. E. Akopyan, V. I. Vovna, *Koordinats. Khim.*[*Coord. Chem.*], 1991, **17**, 1323 (in Russian).
93. V. I. Nefedov, V. I. Vovna, *Elektronnaya struktura khimicheskikh soedineniy* [*Electronic Structure of Chemical Compounds*], Nauka, Moscow, 1987, 347 pp. (in Russian).
94. W. R. Moomaw, D. A. Kleier, J. H. Markgraf, J. W. Thoman, N. A. Ridyard, *J. Phys. Chem.*, 1988, **92**, 4892.
95. T. Kajiwara, S. Masuda, K. Ohno, Y. Harada, *J. Chem. Soc. Perkin Trans.*, 1988, **4**, 507.
96. V. I. Vovna, M. V. Kazachek, I. B. L´vov, *Opt. Spectrosc.*, 2012, **112**, 497.
97. Y. L. Chow, X. Cheng, C. I. Jochansson, *J. Photochem. Photobiol. A*, 1991, **57**, 247.
98. A. G. Mirochnik, B. V. Bukvetskii, E. V. Gukhman, P. A. Zhikhareva, V. E. Karasev, *Russ. Chem. Bull.* (*Int. Ed.*), 2001, **50**, 1612.
99. A. G. Mirochnik, E. V. Fedorenko, D. Kh. Gizzatulina, V. E. Karasev, *Russ. J. Phys. Chem. A*, 2007, **81**, 1880.
100. Y. N. Kononevich, I. B. Meshkov, N. V. Voronina, N. M. Surin, V. A. Sazhnikov, A. A. Safonov, A. A. Bagaturyants, M. V. Alfimov, A. M. Muzafarov, *Heteroat. Chem.*, 2013, **24**, 271.
101. S. Xu, R. E. Evans, T. Liu, G. Zhang, J. N. Demas, C. O. Trindle, C. L. Fraser, *Inorg. Chem.*, 2013, **52**, 3597.
102. S. Chibani, A. Charaf-Eddin, B. Mennucci, B. L. Guennic, D. Jacquemin, *J. Chem. Theory Comput.*, 2014, **10**, 805.
103. G. R. Krishna, R. Devarapalli, R. Prusty, T. Liu, C. L. Fraser, *IUCrJ*, 2015, **2**, 611.
104. T. Sagawa, F. Ito, A. Sakai, Y. Ogata, K. Tanaka, H. Ikeda, *Photochem. Photobiol. Sci.*, 2016, **15**, 420.
105. P. S. Rukin, A. Y. Freidzon, A. V. Scherbinin, V. A. Sazhnikov, A. A. Bagaturyants, M. V. Alfimov, *Phys. Chem. Chem. Phys.*, 2015, **17**, 16997.
106. N. Gelfand, A. Freidzon, E. Fedorenko, *J. Mol. Struct.*, 2018, **1151**, 177.
107. J. J. Yeh, I. Lindau, *Atom. Data Nucl. Data*, 1985, **32**, 1.
108. N. Ooi, A. Rairkar, J. B. Adams, *Carbon*, 2006, **44**, 231.
109. E. A. Taft, H. R. Phillipp, *Phys. Rev.*, 1965, **138**, A197.
110. M. V. Kazachek, I. V. Svistunova, *Spectrochim. Acta Part A*, 2015, **148**, 60.
111. L. Asbrink, O. Edqvist, E. Lindholm, L. E. Selin, *Chem. Phys. Lett.*, 1970, **5**, 192.
112. W. V. Niessen, W. P. Kraemer, G. H. F. Diercksen, *Chem. Phys.*, 1979, **41**, 113.
113. J. P. Maier, J.-F. Muller, *Helv. Chim Acta*, 1975, **58**, 1641.

Received December 28, 2017;
in revised form February 14, 2018;
accepted May 22, 2018